Status of breakup reaction theory

K Ogata[1], T Matsumoto[2,3], S Hashimoto[4], K Minomo[1], T Egami[1], Y Iseri[5], M Kohno[6], S Chiba[4], C A Bertulani[7], Y R Shimizu[1], M Kamimura[1,2] and M Yahiro[1]

[1] Department of Physics, Kyushu University, Fukuoka 812-8581, Japan
[2] RIKEN Nishina Center, Wako 351-0198, Japan
[3] Meme Media Laboratory, Hokkaido University, Sapporo 060-8628, Japan
[4] Advanced Science Research Center, Japan Atomic Energy Agency, Ibaraki 319-1195, Japan
[5] Department of Physics, Chiba-Keizai College, Chiba 263-0021, Japan
[6] Physics Division, Kyushu Dental College, Kitakyushu 803-8580, Japan
[7] Department of Physics, Texas A&M University, Commerce, TX 75429, USA

E-mail: ogata@phys.kyushu-u.ac.jp

Abstract. Recent studies on breakup reactions with the continuum-discretized coupled-channels method are reviewed. The topics covered are: four-body breakup processes for ^{6}He induced reaction, dynamical relativistic effects on Coulomb breakup, microscopic description of projectile breakup processes, description of ternary processes (new triple-α reaction rate) and new approach to inclusive breakup processes.

1. Introduction

Breakup reaction is an indispensable tool to extract not only structural information on weakly-bound nuclei but also dynamical properties of reaction systems involving such fragile nuclei. Recently, breakup properties of unstable nuclei have been studied intensively and extensively. Further investigation on breakup phenomena will be performed in the near future at forthcoming RI beam facilities such as FAIR at GSI and FRIB at MSU, and at the brand-new facility RIBF at RIKEN; some results from RIBF have already been reported [1, 2].

The most successful theoretical model to describe breakup reactions of weakly-bound nuclei is the continuum-discretized coupled-channels method (CDCC) [3, 4], which was proposed and developed by Kyushu group about 25 years ago. Recently, some important developments on CDCC have been made. In this paper we review our recent studies with CDCC on breakup reactions in a wide range of incident energies and for various reaction systems. The following five topics are covered:

i. four-body breakup processes for ^{6}He induced reaction,
ii. dynamical relativistic effects on Coulomb breakup,
iii. microscopic description of projectile breakup processes,
iv. description of ternary processes (new triple-α reaction rate),
v. new approach to inclusive breakup processes.

In Sec. 2, a brief introduction to CDCC is described. The aforementioned topics are discussed in Sec. 3 one by one. Finally, we show summary in Sec. 4.

Published under licence by IOP Publishing Ltd

2. The continuum-discretized coupled-channels method (CDCC)

In CDCC [3, 4], the total wave function of the reaction system is expanded in terms of a complete set of the internal states of the projectile (P):

$$\Psi = \phi_0\chi_0 + \int_0^\infty \phi_k\chi_k dk, \tag{1}$$

where ϕ_0 and ϕ_k are the wave functions of P in the ground and continuum states, respectively, and χ's denote the corresponding wave functions between P and the target nucleus (T). k is the momentum that specifies the energy of P; if P has a two-body structure, k is the relative momentum of the constituents of P. We assume in Eq. (1) that P has one bound state just for simplicity.

The most essential assumption of CDCC is the truncation of the continuum of P, with introducing a cutoff momentum $k_{\max}$. Then we discretize the continuum up to $k_{\max}$ into a finite number of states, i.e., discretized continuum states. There are several choices for the discretization method: the average method, the mid-point method and the pseudostate method. The first one that takes an average of the continuum states within a certain range of k has most widely been used.

After the truncation and discretization, we have the CDCC wave function of the reaction system:

$$\Psi^{\rm CDCC} = \sum_{i=0}^{i_{\max}} \hat{\phi}_i\hat{\chi}_i, \tag{2}$$

where i is the index of the ground ($i = 0$) and the discretized continuum ($0 < i \leq i_{\max}$) channels; the symbol $\hat{}$ denotes a result of discretization.

In CDCC, we assume that the set of $\{\hat{\phi}_i\}$, which defines the modelspace of CDCC, forms a complete set in the space that is significant for a reaction process considered. In other words, the CDCC wave function is not exact in entire space but can be used as an exact solution in evaluation of physics observables; note that a transition matrix contains a residual interaction that has a finite range. Thus, as mentioned in the review article [5], the modelspace of CDCC depends in general on the type of the reaction, the physics quantities to be calculated, the incident energy, outgoing angle, etc. of observation, and also the desired accuracy of the calculation. One can see that CDCC is an effective reaction model designed to describe physics observables with sufficiently high but limited accuracy. Note, however, that the theoretical foundation of CDCC has been established in connection with the distorted-wave Faddeev equation in [6, 7], and a solution of CDCC is shown to have a proper asymptotic form in [8].

3. Breakup reaction studies with CDCC

In this section, we review our recent works very briefly. See the references cited in the following subsections for the details of the formalism, numerical calculation, other results and further discussion.

3.1. Four-body breakup processes for ^{6}He induced reaction

To describe a breakup process of a three-body projectile like ^{6}He, we need discretized continuum states of the three-body system. It is very difficult to obtain them by directly solving a three-body scattering problem. However, if we diagonalize a Hamiltonian of ^{6}He, we automatically obtain the eigenstates both below and above the three-body threshold energy. The latter states (the pseudostates) can be assumed as discretized continuum states. Thus, we obtain the total wave function of the four-body system, i.e., the three-body projectile and the target nucleus, in terms of finite number of channels. This four-body CDCC was established in [9]; for the

calculation of ^{6}He wave functions, the Gaussian expansion method [10] that has been highly successful in few-body physics is adopted.

Four-body CDCC is applied to the ^{6}He elastic scattering by ^{209}Bi near the Coulomb barrier energy [11]. Figure 1 shows the elastic differential cross section (in ratio to the Rutherford cross

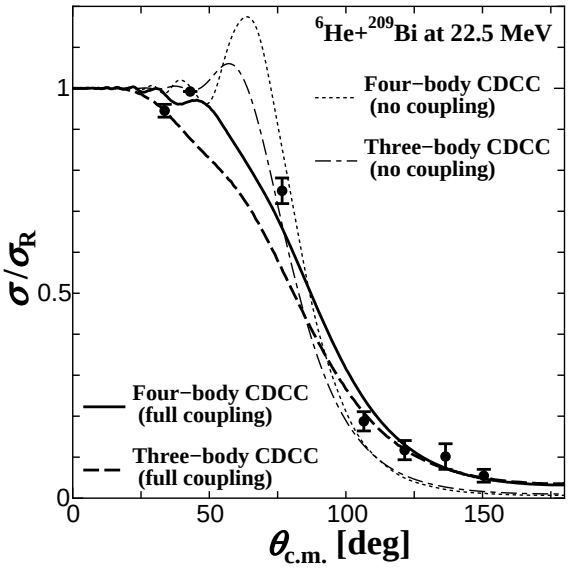

Figure 1. Angular distribution of the elastic differential cross section as the ratio to the Rutherford cross section for the ^{6}He+^{209}Bi scattering at 22.5 MeV. The solid (dashed) and dotted (dot-dashed) lines show the results of the four-body CDCC (three-body CDCC) calculation with and without breakup effects, respectively. The experimental data are taken from [12, 13]. We take the incident energy of 22.5 MeV shown in the first paper of Aguilera *et al.* [12].

section) at 22.5 MeV, as a function of the center-of-mass scattering angle. The solid line is the result of four-body CDCC and the dashed line is that of three-body CDCC based on a naive dineutron model for ^{6}He. One sees that four-body CDCC reproduces the experimental data

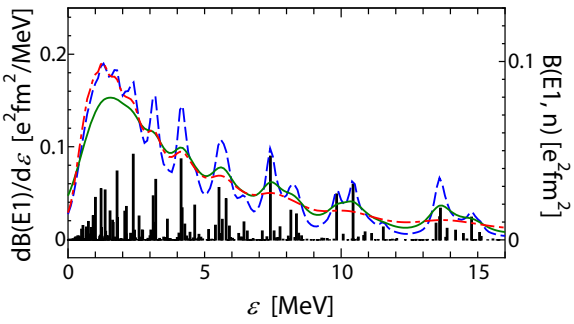

Figure 2. E1 strength distribution of ^{6}He as a function of ϵ. The bars show $B(\mathrm{E1}; n)$ from the 0^+ ground state to the nth pseudostates of ^{6}He. The solid, dashed and dash-dotted lines respectively show the smeared E1 strength distributions assuming the Lorentzian form with the width of 0.5, 0.2 and $0.1(\epsilon_n + 0.975)$ MeV; ϵ_n denotes the eigenenergy of the nth pseudostate.

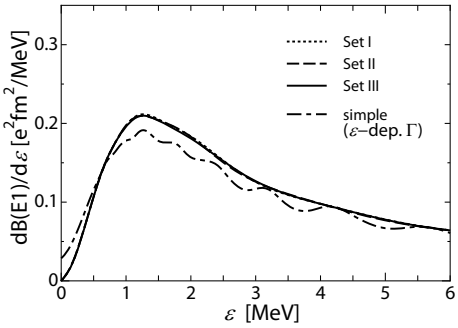

Figure 3. E1 strength distribution of ^{6}He as a function of ϵ obtained with the smoothing method in [17]. The dotted, dashed and solid lines show the results with different modelspace of the ^{6}He wave function (see [17] for details). Also shown for comparison by the dot-dashed curve is the result of the simple smoothing method with a energy-dependent width, i.e., the dash-dotted line in Fig. 2.

[12, 13] well, while three-body CDCC does not. The results of four-body CDCC and three-body CDCC without breakup effects of ^{6}He are shown by the dotted and dot-dashed lines, respectively. The difference between the solid and dotted (dashed and dot-dashed) lines shows effects of the four-body (three-body) breakup on the elastic cross section. The breakup effects on the elastic cross section, i.e., virtual breakup processes, are found to be very important in this reaction.

Recently, Rodríguez-Gallardo and collaborators [14] developed an alternative four-body CDCC, with directly calculating three-body scattering states of ^{6}He. The method also reproduces well the elastic cross section of ^{6}He on ^{208}Pb near the Coulomb barrier energy. As future work, systematic analysis of four-body breakup will be necessary. Another important subject is the extension of four-body CDCC to 5- and 6-body reaction systems; we are planning to achieve this by incorporating cluster-orbital shell-model (COSM) wave functions [15, 16].

Description of breakup spectrum is a hot topic of four-body CDCC. Since CDCC uses discretized continuum states, the resulting breakup cross sections are discrete. In Fig. 2 we show by histogram a typical example of the discrete result of the energy distribution of the electric dipole (E1) strength $dB(\mathrm{E1})/d\epsilon$ for ^{6}He, with ϵ the breakup energy of ^{6}He measured from the three-body ($^4\mathrm{He}+n+n$) threshold. To compare the result of CDCC with experimental data, we must construct a smooth spectrum from the histogram. Note that a simple smearing procedure assuming a Lorentzian form, with any choice of parameters, does not work at all, as shown by the three lines in Fig. 2. Thus, we proposed a new smoothing method with the use of the Lippmann-Schwinger equation [17], which was found to successfully reproduce a smooth $dB(\mathrm{E1})/d\epsilon$, if experimental resolution was taken into account; the result is shown in Fig. 3.

The alternative four-body CDCC [14] can construct a smooth spectrum of breakup observable much easier, in principle, than the original four-body CDCC, since in the former the three-body scattering states are directly calculated. At this stage, however, because of the limited modelspace, it seems difficult to compare the result shown in [14] with experimental data. Very recently, another smoothing procedure using the complex scaling method [18, 19] has been proposed in [20] and shown to work very well to obtain smooth breakup cross sections.

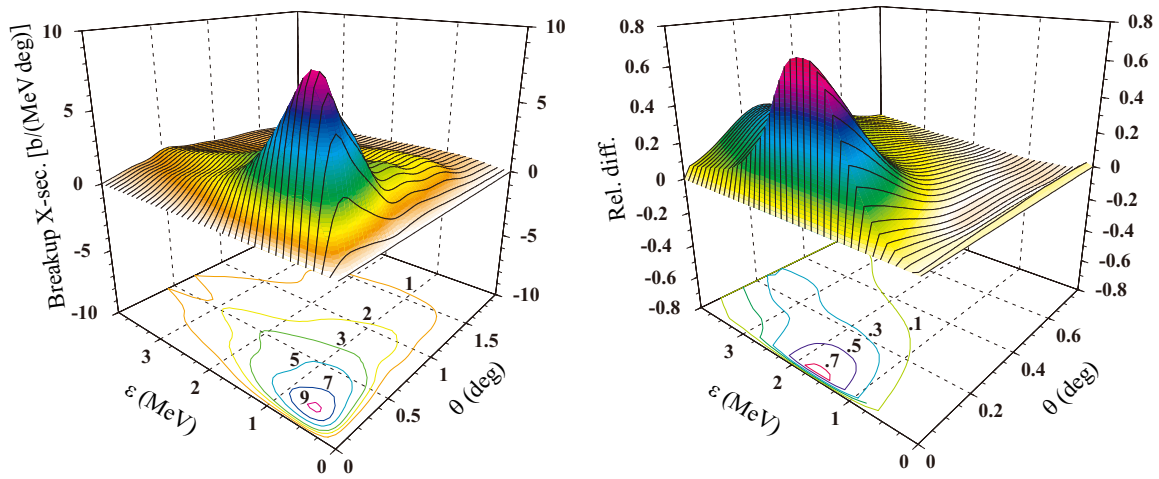

Figure 4. Double differential breakup cross section for ^{8}B+^{208}Pb at 250 MeV/nucleon including dynamical relativistic corrections (left panel) and its relative difference from the calculation without relativistic corrections (right panel).

3.2. Dynamical relativistic effects on Coulomb breakup

When one deals with a process at intermediate energies, kinematical correction due to relativity is usually included. What we propose here is to directly include relativistic Coulomb interaction, i.e., the Liénard-Wiechert potential. It should be noted that this is usually done in calculation with a virtual photon theory. However, inclusion of the relativistic Coulomb interaction in CDCC has not been done.

In [21] and [22], a new version of CDCC incorporating the Liénard-Wiechert potential is developed. The left panel of Fig. 4 shows the double differential breakup cross section of ^{8}B by ^{208}Pb at 250 MeV per nucleon. θ is the scattering angle of the center mass of ^{7}Be and p, and ϵ is the breakup energy between the two fragments. In the right panel, the relative difference between the relativistic and nonrelativistic results is shown. One sees significant increase in the cross section of several tens of percent level. It should be noted that this dynamical relativistic effects are important not in the tail of the cross section but near the peak. Thus, we conclude that the relativistic treatment of Coulomb interaction is necessary to analyze Coulomb breakup processes at intermediate energies to be measured in the new and forthcoming RI beam facilities.

3.3. Microscopic description of projectile breakup processes

An essential ingredient of CDCC for systematic analysis of breakup reactions is optical potentials between A and individual constituents of P, which are not always available phenomenologically. Thus, we need a microscopic framework to obtain optical potentials for various reaction systems in a wide range of incident energies.

For nucleon-nucleus potential, the method proposed by Brieva and Rook [23, 24, 25] has widely been used to obtain a microscopic local potential. Recently, it has been shown in [26] that the Brieva-Rook (BR) localization is valid for wide range of incident energies, by directly comparing the result of BR calculation with the solution of the exact nonlocal Schrödinger equation. In Fig. 5 we show the elastic differential cross sections of the proton scattering on

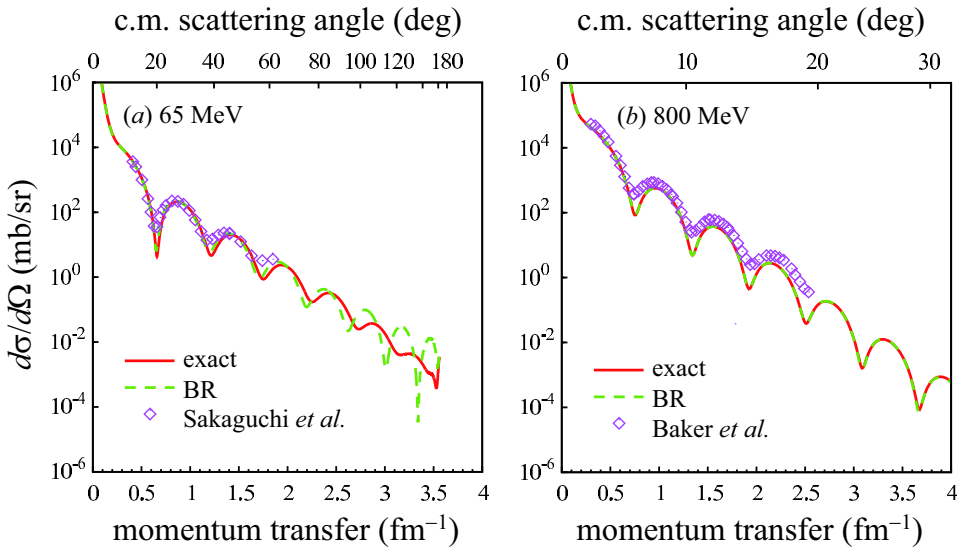

Figure 5. The elastic differential cross sections of the proton scattering on ^{90}Zr at (a) 65 MeV and (b) 800 MeV. The solid lines represent the results of the exact calculation, while the dashed lines show the results of the calculation with the BR localization. Experimental data are taken from [29, 30].

^{90}Zr at (a) 65 MeV and (b) 800 MeV. The solid and dashed lines respectively show the results of the exact calculation and the BR localization.

For nucleus-nucleus potentials, Furumoto and the collaborators [27] have done intensive study with proposing a new nucleon-nucleon g matrix [28] that contains three-body force effects phenomenologically.

Therefore, we are ready for systematic analysis of experimental data of breakup processes of unstable nuclei. We call CDCC with microscopic optical potentials microscopic CDCC.

3.4. Description of ternary processes (new triple-α reaction rate)

In this subsection, the description of ternary processes, in which there are three incident particles, is discussed. The ternary process can be considered to be a reaction process that begins with an unbound state of a two-body projectile. In this sense, it is closely related to the breakup reaction theory.

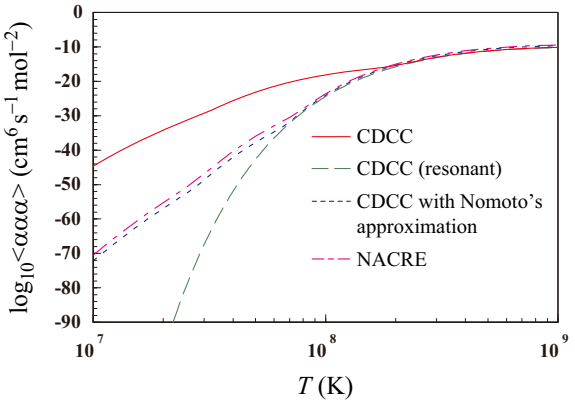

Figure 6. Triple-α reaction rate as a function of temperature. The solid line represents the result of CDCC. The dashed line shows the contribution of resonant capture. The result of CDCC with Nomoto's approximation is shown by the dotted line. The dash-dotted line shows the reaction rate of NACRE [32].

In [31], formulation of the ternary process based on CDCC is developed, and applied to the study of the triple-α reaction. We describe resonant and nonresonant processes on the same footing. Figure 6 shows the resulting reaction rate. The horizontal axis is temperature and the vertical axis is the order of the rate. The solid line is the new reaction rate calculated with CDCC, which is much larger than the rate of NACRE [32] shown by the dash-dotted line. The difference is up to about 20 orders of magnitude around 10^7 K. We stress that it is shown in [31] that the method for describing three-particle processes proposed by Nomoto [33, 34], Nomoto's method, that has widely been used in nuclearastrophysical studies including the NACRE compilation, is very crude, and even unphysical. This can be understood clearly if one sees the reaction probability $(\sigma v)_{\epsilon 1,E}$, where ϵ_1 is the α-α relative energy and E is the total energy of the three-α system. The solid line in Fig. 7 shows $(\sigma v)_{\epsilon 1,E}$ for $\epsilon_1 = 38.2$ keV, which corresponds to the nonresonant α-α state below the α-α resonance at 92.0 keV, calculated with CDCC. On the other hand, in Nomoto's method, the probability shown by the dashed line is used. One sees that it has a resonance peak at different energy from that of the Holye state ($E = 387$ keV). This is the same as at different ϵ_1. Therefore, one finds that Nomoto's method implicitly assumes that there are infinite number of resonances around the Hoyle resonance, which is obviously inconsistent with the experimental information on ^{12}C. Furthermore, if we adopt in our CDCC calculation the unphysical assumption used in Nomoto's method (and also in NACRE), we obtain the reaction rate shown by the dotted line in Fig. 6 that agrees well with the rate of NACRE.

We stress that the calculation of the triple-α reaction at low energies requires extremely large modelspace as described in [31]. We have confirmed a clear convergence of the reaction rate with

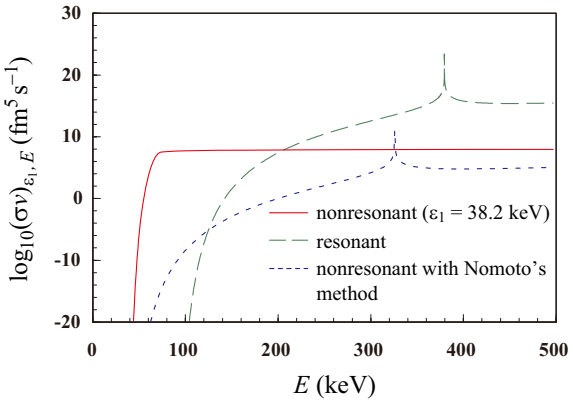

Figure 7. The solid and dashed lines show the reaction probability $(\sigma v)_{\epsilon_1,E}$ for the nonresonant ($\epsilon_1 = 38.2$ keV) and resonant processes, respectively. The dotted line shows the result for the nonresonant process with Nomoto's approximation in CDCC calculation.

respect to the modelspace of CDCC; the maximum value $r_{\max}$ of the α-α relative coordinate r is set to 5,000 fm. If r is truncated at a smaller value, say, 200 fm, we have a reaction rate much smaller than the rate shown by the solid line in Fig. 6, by about 6 orders of magnitude at 10^8 K. It is also found that one channel calculation never converges, and an adiabatic description of the three-particle system at low energies does not work at all. More detailed analysis of the triple-α process with CDCC will be shown in a forthcoming paper.

In [35], it is reported that a stellar evolution model computed with our new triple-α reaction rate causes inconsistency with the observations of red giant branches; they have no such a problem when the triple-α reaction rate of NACRE is adopted. Since we have clarified that the description of the nonresonant triple-α process in NACRE has no theoretical foundation, further investigation on what causes the inconsistency in [35] will be very interesting and important.

Very recently, our new reaction rate has been applied to study on Cepheids [36]. It is shown that if our new reaction rate is slightly tuned, a long-standing problem between calculation and observation on Cepheids can be resolved, which clearly shows the importance of the increase in the triple-α reaction rate around 10^8 K, compared with the rate of NACRE.

3.5. New approach to inclusive breakup processes

Let us consider the ^{7}Li(d, nx) reaction. Here x means that the final state except for the neutron is not specified. This inclusive breakup process is called also a stripping or incomplete fusion process. In [37] we propose a new method to describe the inclusive breakup cross section with decomposing the total fusion cross section:

$$\sigma_{\rm TF} = \frac{2\mu}{\hbar^2 K} \left| \langle \Psi \left| -W_p - Wn \right| \Psi \rangle \right| . \tag{3}$$

In Eq. (3), Ψ is the total wave function of the $p + n$+^{7}Li three body system calculated with CDCC, μ and K are, respectively, the reduced mass and relative momentum between d and ^{7}Li, and W_p (W_n) is the imaginary part of the proton (neutron) optical potential for ^{7}Li. In [37], we divide the integration region into four:

$$\begin{aligned} \int d\mathbf{r}_p \int d\mathbf{r}_n \;=\; & \int_{r_p<r_p^{\rm ab}} d\mathbf{r}_p \int_{r_n<r_p^{\rm ab}} d\mathbf{r}_n + \int_{r_p<r_p^{\rm ab}} d\mathbf{r}_p \int_{r_n>r_p^{\rm ab}} d\mathbf{r}_n \\ & + \int_{r_p>r_p^{\rm ab}} d\mathbf{r}_p \int_{r_n<r_p^{\rm ab}} d\mathbf{r}_n + \int_{r_p>r_p^{\rm ab}} d\mathbf{r}_p \int_{r_n>r_p^{\rm ab}} d\mathbf{r}_n , \end{aligned} \tag{4}$$

with introducing absorbing radii for proton ($r_p^{\rm ab}$) and neutron ($r_n^{\rm ab}$). The first term on the right-hand-side (r.h.s.) of Eq. (4) corresponds to the process in which both proton and neutron

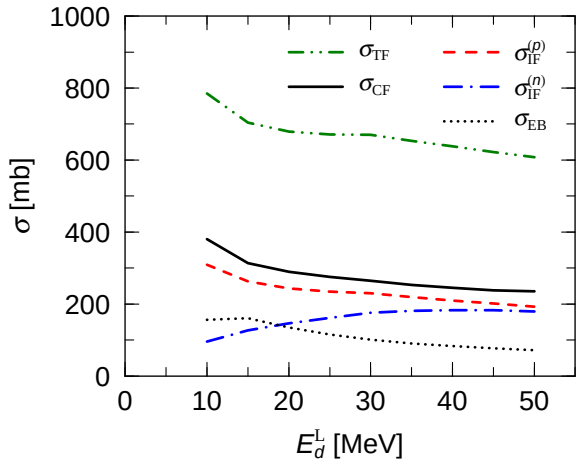

Figure 8. Results of the total fusion cross section $\sigma_{\rm TF}$ (dash-double-dotted line), complete fusion cross section $\sigma_{\rm CF}$ (solid line), proton-absorbed cross section $\sigma_{\rm IF}^{(p)}$ (dashed line) and neutron-absorbed cross section $\sigma_{\rm IF}^{(n)}$ (dash-dotted line) for the deuteron induced reaction on ^{7}Li as a function of the deuteron incident energy $E_d^{\rm L}$. The dotted line represents the elastic breakup cross sections calculated with CDCC.

are absorbed. The second (third) term on r.h.s. represents the process in which only proton (neutron) is absorbed. Note that the contribution of the fourth term is negligible. Thus, if we take just the second term, we can obtain the cross section of the inclusive (d, nx) process.

The point is how to determine the absorbing radii. In [37] we use the result of theoretical analysis of the ^{7}Li(d, nx) reaction at 40 MeV; we analyzed in [38] the double differential cross section data [39] by summing up the elastic breakup cross section calculated with CDCC and the stripping cross section calculated with the Glauber model. The data are reproduced very well with no free parameter, except for the contribution of the preequilibrium and evaporation processes that are negligible where the stripping process is important. Thus, we conclude that the integrated value of the stripping cross section calculated with the Glauber model can be regarded as an experimental value. The absorbing radii are fixed to reproduce this value at 40 MeV.

We show in Fig. 8 the result of the inclusive breakup cross sections as a function of the deuteron incident energy. The dashed (dash-dotted) line shows the proton-absorbed (neutron-absorbed) cross section and the solid line is the complete fusion cross section. These three values are comparable above 30 MeV, and much larger than the elastic breakup cross section shown by the dotted line. Another finding is the energy dependence of the dashed and dash-dotted lines is very different at low energies. This difference comes from different energy dependence of the

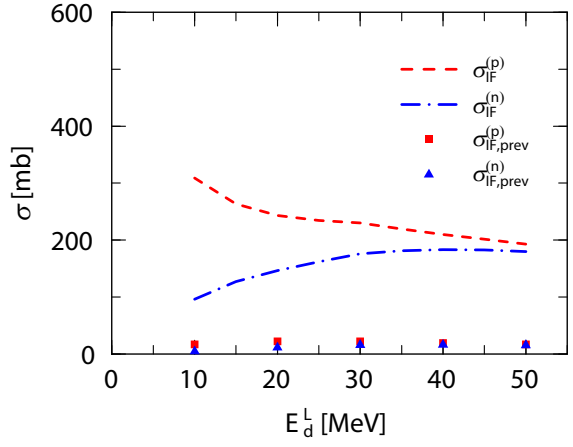

Figure 9. $\sigma_{\rm IF}^{(p)}$ (dashed line) and $\sigma_{\rm IF}^{(n)}$ (dash-dotted line) calculated with the present method, compared with $\sigma_{\rm IF,prev}^{(p)}$ (squares) and $\sigma_{\rm IF,prev}^{(n)}$ (triangles) following the previous definition given in Refs. [42] and [43].

proton and neutron optical potentials [40, 41] adopted. In Fig. 9 we show the comparison between our results and the results based on the method proposed by Diaz-Torres and Thompson [42] and Iijima [43]. The preceding method assumes that the three-body wave function corresponding to breakup channels are only responsible to the inclusive breakup, or incomplete fusion. However, the method is found to give much smaller cross sections than the present calculation. Since our result at 40 MeV is fitted to the experimental value, we can conclude that the previous method does not work, at least for the ^{7}Li(d, nx) process at 40 MeV. Description of the double-differential cross sections of inclusive processes with CDCC will be important future work.

4. Summary

In the present paper, some recent studies on breakup reactions by means of the continuum-discretized coupled-channels method (CDCC) are briefly reviewed. Future plans described in the preceding subsections will be very important for theoretical nuclear reaction studies. Another topic to be addressed is the quantitative description of transfer reactions. Recently, numerical comparison between the results of CDCC and Faddeev for various reactions was reported [44]; there remains a significant difference only for a transfer process. More accurate description of transfer reactions with CDCC than in [44] will be an interesting and important subject in future.

Acknowledgments

K. O. acknowledges M. Kawai for fruitful discussions. This work has been supported in part by the Grants-in-Aid for Scientific Research of Monbukagakusyou of Japan.

References

[1] Nakamura T *et al.*, 2010 *Phys. Rev. Lett.* **103** 262501
[2] Doornenbal P, Scheit H, Kobayashi N, Aoi N, Takeuchi S, Li K, Takeshita E, Togano Y, Wang H, Deguchi S, Kawada Y, Kondo Y, Motobayashi T, Nakamura T, Satou Y, Tanaka K N and Sakurai H 2010 *Phys. Rev.* C **81** 041305(R)
[3] Kamimura M, Yahiro M, Iseri Y, Sakuragi Y, Kameyama H and Kawai M 1986 *Prog. Theor. Phys. Suppl.* **89** 1
[4] Austern N, Iseri Y, Kamimura M, Kawai M, Rawitscher G and Yahiro M 1987 *Phys. Rep.* **154** 125
[5] M. Kawai, 1986 *Prog. Theor. Phys. Suppl.* **89** 11
[6] Austern N, Yahiro M and Kawai M 1989 *Phys. Rev. Lett.* **63** 2649
[7] Austern N, Kawai M and Yahiro M 1996 *Phys. Rev.* C **53** 314
[8] Piyadasa R A D, Kawai M, Kamimura M and Yahiro M 1999 *Phys. Rev.* C **60** 044611
[9] Matsumoto T, Hiyama E, Ogata K, Iseri Y, Kamimura M, Chiba S and Yahiro M 2004 *Phys. Rev.* C **70** 061601(R)
[10] Hiyama E, Kino Y and Kamimura M 2003 *Prog. Part. Nucl. Phys.* **51** 223
[11] Matsumoto T, Egami T, Ogata K, Iseri Y, Kamimura M and Yahiro M 2006 *Phys. Rev.* C **73** 051602(R)
[12] Aguilera E F, Kolata J J, Nunes F M, Becchetti F D, DeYoung P A, Goupell M, Guimarães V, Hughey B, Lee M Y, Lizcano D, Martinez-Quiroz E, Nowlin A, O'Donnell T W, Peaslee G F, Peterson D, Santi P and White-Stevens R 2000 *Phys. Rev. Lett.* **84** 5058
[13] Aguilera E F, Kolata J J, Becchetti F D, DeYoung P A, Hinnefeld J D, Horváth Á, Lamm L O, Lee H-Y, Lizcano D, Martinez-Quiroz E, Mohr P, O'Donnell T W, Roberts D A and Rogachev G 2001 *Phys. Rev.* C **63** 061603(R)
[14] Rodríguez-Gallardo M, Arias J M, Gómez-Camacho J, Moro A M, Thompson I J and Tostevin J A 2009 *Phys. Rev.* C **80** 051601(R)
[15] Suzuki Y and Ikeda K 1988 *Phys. Rev.* C **37** 410
[16] Aoyama S, Myo T, Katō K and Ikeda K 2006 *Prog. Theor. Phys.* **116** 1
[17] Egami T, Matsumoto T, Ogata K and Yahiro M 2009 *Prog. Theor. Phys.* **121** 789
[18] Aguilar J and Combes J M 1971 *Commun. Math. Phys.* **22** 269
[19] Balslev E and Combes J M 1971 *Commun. Math. Phys.* **22** 280
[20] Matsumoto T, Katō K and Yahiro M 2010 *Phys. Rev.* C **82** 051602(R)
[21] Ogata K and Bertulani C A 2009 *Prog. Theor. Phys.* **121** 1399
[22] Ogata K and Bertulani C A 2010 *Prog. Theor. Phys.* **123** 701
[23] Brieva F A and Rook J R 1977 *Nucl. Phys.* A **291** 299

[24] Brieva F A and Rook J R 1977 *Nucl. Phys.* A **291** 317
[25] Brieva F A and Rook J R 1978 *Nucl. Phys.* A **297** 206
[26] Minomo K, Ogata K, Kohno M, Shimizu Y R and Yahiro M 2010 *J. Phys.* G **37** 085011
[27] Furumoto T, Sakuragi Y and Yamamoto Y 2009 *Phys. Rev.* C **79** 011601(R)
[28] Furumoto T, Sakuragi Y and Yamamoto Y 2008 *Phys. Rev.* C **78** 044610
[29] Sakaguchi H, Nakamura M, Hatanaka K, Goto A, Noro T, Ohtani F, Sakamoto H, Ogawa H and Kobayashi S, 1982 *Phys. Rev.* C **26** 944
[30] Baker F T, Scott A, Grimm M A, Love W G, Penumetcha V, Glashausser C, Adams G S, Igo G, Hoffmann G W, Moss J M, Swenson W and Wood B E 1983 *Nucl. Phys.* A **393** 283
[31] Ogata K, Kan M and Kamimura M 2009 *Prog. Theor. Phys.* **122** 1055
[32] Angulo C *et al.* 1999 *Nucl. Phys.* A **656** 3
[33] Nomoto K 1982 *Astrophys. J.* **253** 798
[34] Nomoto K, Thielemann F-K and Miyaji S 1985 *Astron. Astrophys.* **149** 239
[35] Dotter A and Paxton B 2009 *Astron. Astrophys.* **507** 1617
[36] Morel P, Provost J, Pichon B, Lebreton Y and Thévenin F 2010 *Astron. Astrophys.* **520** A41
[37] Hashimoto S, Ogata K, Chiba S and Yahiro M 2009 *Prog. Theor. Phys.* **122** 1291
[38] Ye T, Watanabe Y and Ogata K, 2009 *Phys. Rev.* C **80** 014604
[39] Hagiwara M, Itoga T, Kawata N, Hirabayashi N, Oishi T, Yamauchi T, Baba M, Sugimoto M and Muroga T 2005 *Fusion Sci. Technol.* **48** 1320
[40] Chiba S, Togasaki K, Ibaraki M, Baba M, Matsuyama S, Hirakawa N, Shibata K, Iwamoto O, Koning A J, Hale G M and Chadwick M B 1998 *Phys. Rev.* C **58** 2205
[41] Ye T, Watanabe Y, Ogata K and Chiba S 2008 *Phys. Rev.* C **78** 024611
[42] Diaz-Torres A and Thompson I J 2002 *Phys. Rev.* C **65** 024606
[43] Iijima M, Aoki Y, Ozawa A and Okumura N 2007 *Nucl. Phys.* A **793** 79
[44] Deltuva A, Moro A M, Cravo E, Nunes F M and Fonseca A C 2007 *Phys. Rev.* C **76** 064602